
Multilingual OCR-Aware Fine-Tuning and Prompt-Guided Chain-of-Thought Reasoning for Multimodal Large Language Models

Qinwu Xu¹ Yifan Jiang² Haoyu Ren^{1,*}

¹Meta AI

²UT Austin

* Current independent researcher

Abstract

Optical character recognition (OCR) and multilingual text understanding remain major failure modes of multimodal large language models (MLLMs), particularly in real-world images containing cluttered layouts, small fonts, blur, occlusion, and complex typography.

We present an OCR-aware multilingual multimodal training framework that combines (i) large-scale synthetic OCR-to-translation data generation, (ii) OCR-aware supervised fine-tuning (SFT) with LoRA adaptation, and (iii) structured visual chain-of-thought (CoT) prompting for reasoning under uncertain visual conditions. Using a LLaMA-based multimodal architecture, the proposed framework substantially improves OCR completeness, multilingual translation accuracy, and robustness under degraded visual conditions.

Experimental results on multilingual receipts, menus, posters, signs, handwritten text, and document images demonstrate significantly improved visual-text grounding compared with the baseline model. In particular, the proposed OCR-aware post-training framework improves extraction of small, blurred, spatially scattered, and partially occluded text while reducing reliance on language priors under uncertain OCR conditions. Qualitative comparisons with frontier multimodal systems, including GPT-5-class and Gemini-family models, further suggest improved OCR grounding and reduced hallucination under noisy and visually ambiguous OCR scenarios.

Overall, the results indicate that data-centric OCR-aware multimodal post-training provides an effective and scalable direction for improving multilingual OCR and OCR-based visual question answering systems.

1 Introduction

1.1 Background

Text in images is ubiquitous in real-world environments, including menus, receipts, medication labels, street signs, posters, and official documents. Correctly reading and translating such text is essential for multimodal assistants and assistive AI systems. However, OCR in natural images remains fundamentally more challenging than traditional document OCR due to blur, glare, perspective distortion, partial occlusion, cluttered layouts, and multilingual scripts.

Despite substantial progress in vision-language models (VLMs), including LLaVA, Qwen-VL, PaLI-X, Kosmos-2, Gemini-family models, LLaMA-family multimodal systems, and GPT-4 and 5-class multimodal models, these systems still frequently hallucinate text, omit crucial tokens, or generate mistranslations under degraded visual conditions. Even models achieving strong bench-

40th Conference on Neural Information Processing Systems (NeurIPS 2026).

mark performance on datasets such as TextVQA and DocVQA may struggle for in-the-wild scenarios.

In practice, we observe several recurring failure modes:

- (i) Small or degraded text may be skipped or inaccurately recognized.
- (ii) OCR content distributed across multiple image regions may be only partially extracted.
- (iii) Partially visible text may be autoregressively “completed” using language priors rather than grounded visual evidence.
- (iv) Numeric values may be hallucinated.
- (v) Multilingual translations may drift when OCR uncertainty is high.

Recent frontier multimodal systems partially mitigate some of these issues through explicit visual reasoning and tool-augmented inference strategies that analyze visible text before generating responses. However, such reasoning pipelines are often computationally expensive in large-scale settings .

1.2 Objective

This paper investigates whether OCR robustness and multilingual text understanding in multimodal large language models (MLLMs) can be substantially improved through OCR-aware data curation and supervised post-training.

We introduce two complementary approaches:

- (i) OCR-aware post-training using multilingual OCR datasets with LoRA-based supervised fine-tuning (SFT).
- (ii) A lightweight visual chain-of-thought (CoT) prompting strategy that provides auxiliary structured reasoning over visible text regions.

2 Related Work

2.1 OCR-Capable Multimodal Large Language Models

Recent multimodal large language models (MLLMs), including Qwen-VL (Bai 2023), PaLI-X (chen 2023), LLaVA (Liu 2023), Kosmos-2 (Peng 2023), and mPLUG-Owl (Ye 2023), integrate visual encoders with large language models to enable multimodal understanding and OCR-related reasoning. Although these systems demonstrate strong performance on multimodal benchmarks, they often remain sensitive to visual degradation such as blur, rotation, occlusion, cluttered layouts, and multilingual text, leading to incomplete OCR extraction and hallucinated text generation.

2.2 Document and Scene-Text Benchmarks

Benchmarks such as TextVQA (Singh 2019) and DocVQA (Mathew 2021) evaluate multimodal reasoning over scene text and document images. While these datasets significantly advanced OCR-oriented multimodal evaluation, they under-represent challenging in-the-wild conditions including severe blur, low-light imaging, perspective distortion, multilingual text mixtures, and scattered OCR regions commonly observed in mobile-camera environments.

2.3 Visual Reasoning and Chain-of-Thought Prompting

Recent multimodal systems have explored reasoning-guided inference strategies for improving OCR and visual understanding. Chain-of-thought (CoT) prompting (Wei 2022) chain-of-thought and multimodal reasoning frameworks such as MM-ReAct (Yang 2023) and Visual ChatGPT (Wu 2023) incorporate structured reasoning or external visual tools to improve perception under ambiguous visual conditions. However, these approaches are often computationally expensive and difficult to deploy efficiently at scale.

2.4 Data-Centric Multimodal Alignment

Recent work has increasingly emphasized the importance of data-centric post-training, synthetic instruction generation, and preference optimization for improving multimodal grounding and reducing hallucination (Wang 2023, Rafailov 2023). Our work follows this direction by focusing on OCR-aware multilingual data curation and supervised multimodal post-training to improve OCR completeness, translation robustness, and hallucination reduction under degraded visual conditions.

3 Methodologies

3.1 Model Architecture

We adopt an existing multimodal vision-language model (VLM) architecture inspired by recent large-scale systems such as AnyMal (Moon et al., 2024), Flamingo (Alayrac et al., 2022), and BLIP-2 (Li et al., 2023), with LLaMA-3 70B serving as the language backbone. Our work does not introduce a new multimodal architecture, additional OCR-specific recognition modules, or external OCR engines.

Given an input image, a frozen MetaCLIP-based ViT encoder (Xu et al., 2023) extracts dense visual features, which are compressed into a fixed number of visual tokens through a Perceiver-based resampling module (Jaegle et al., 2021). The visual tokens are aligned with the language embedding space and concatenated with text tokens before being processed by the LLaMA decoder for end-to-end multimodal reasoning and generation, as illustrated in Figure 1.

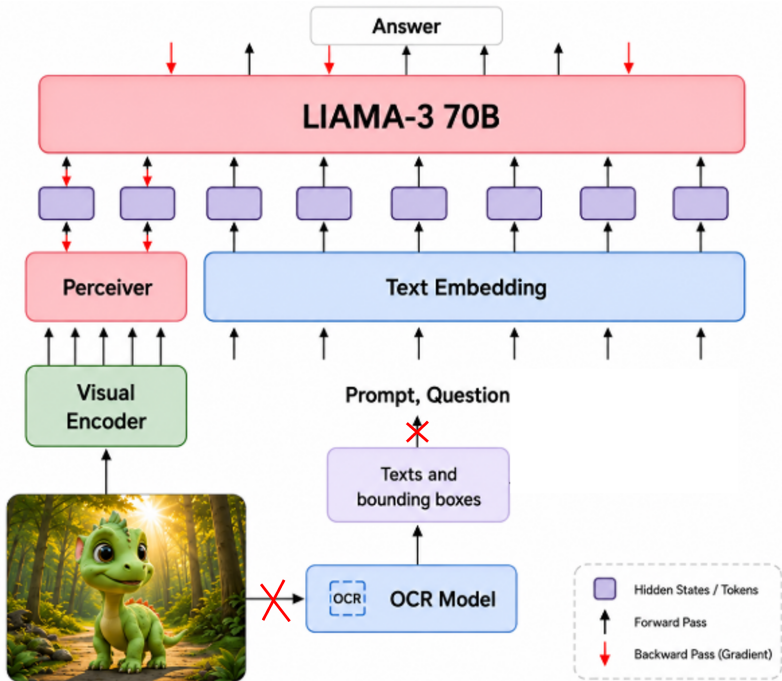


Figure 1: Model architecture: image features are embedded and aligned with text tokens as inputs to the LLaMA decoder for multimodal generation. During training, the LLaMA and Perceiver module weights are updated through backpropagation, while the ViT encoder remains frozen. Our framework does not rely on an external OCR model.

Comparison with traditional OCR-based pipelines. Conventional vision-language systems often rely on a modular OCR-centric pipeline, where text understanding is delegated to a dedicated OCR subsystem. This typically involves a multi-stage process: (i) text detection (e.g., EAST (Zhou et al., 2017), CRAFT (Baek et al., 2019)), (ii) text recognition (e.g., Tesseract (Smith, 2007), TrOCR (Li et al., 2021)), and (iii) structured encoding of recognized text (often including bounding boxes or layout metadata) before feeding into an LLM or downstream reasoning model. In some systems, external OCR services such as Google Vision OCR are also used as black-box components.

While effective, such pipelines introduce several limitations, including increased latency, error propagation across stages, and sensitivity to noisy or redundant detections (e.g., over-fragmented bounding boxes or spurious text regions). Moreover, decoupling perception from reasoning can hinder joint optimization across modalities.

Unlike some existing LLaMA3-based OCR systems that incorporate an additional OCR model for explicit text extraction before LLM reasoning, our framework removes the separate OCR module and learns OCR capability directly within the end-to-end multimodal model through OCR-aware post-training. This end-to-end design reduces system complexity, improves robustness to noisy visual inputs, and enables tighter coupling between visual perception and language reasoning.

3.2 Problem Formulation

We study multimodal reasoning in vision-language models under noisy OCR conditions, where textual information is implicitly embedded within visual inputs and must be inferred from degraded observations.

Let I denote an image, Z latent OCR regions (e.g., text bounding boxes), T the underlying text extracted from those regions, and Y the target output (e.g., answer or translation). The overall task can be modeled as marginalizing over latent textual structure:

$$p(Y | I) = \sum_Z p(Y | T(Z), I) p(Z | I) \quad (1)$$

This formulation highlights a key source of uncertainty: OCR is not directly observed but must be inferred via $p(Z|I)$, which becomes increasingly unreliable under visual degradation (e.g., blur, occlusion, perspective distortion). As a result, errors in latent text extraction propagate to downstream reasoning, and the model must operate under a highly uncertain latent-text bottleneck.

In practice, modern multimodal language models approximate this distribution implicitly via autoregressive decoding:

$$p(Y | I, q) = \prod_t p(y_t | y_{<t}, I, q), \quad (2)$$

where q denotes the query. However, this factorization introduces a known limitation: when visual evidence is weak, the model may rely disproportionately on learned language priors rather than grounded OCR signals, leading to hallucinated or partially inferred text.

Under visually degraded conditions, uncertainty in $p(Z|I)$ increases, making reliable text grounding difficult and effectively weakening the connection between visual input and linguistic output. This mismatch between latent visual uncertainty and strong autoregressive priors is a primary driver of OCR omission and hallucination errors.

To address this issue, the model is first optimized using supervised fine-tuning (SFT):

$$\mathcal{L}_{\text{SFT}} = -\log p_{\theta}(Y | I, q), \quad (3)$$

which learns direct mappings from visual inputs to target outputs at scale. In most OCR scenarios, this objective provides strong multimodal alignment and constitutes the primary source of performance improvement in our framework.

However, under visually ambiguous or heavily degraded OCR conditions, directly modeling $p(Y | I, q)$ can still be challenging, as uncertainty in latent OCR regions may propagate through autoregressive decoding. In such cases, the model may partially rely on dominant language priors when visual evidence is incomplete or noisy.

3.3 Visual CoT Prompting

To improve robustness under these challenging conditions, we additionally incorporate visual prompt chain-of-thought (CoT) reasoning as an auxiliary grounding mechanism. This motivates the introduction of reasoning-based supervision, where the model is encouraged to explicitly construct intermediate visual evidence before producing the final answer. We implement this using visual prompt CoT, introducing a latent reasoning trace R :

$$p(Y | I, q) = \sum_R p_{\theta}(Y | R, I, q) p_{\theta}(R | I, q). \quad (4)$$

Rather than directly generating the final output from uncertain visual observations, the model first predicts an intermediate reasoning process:

$$R \sim p_{\theta}(R | I, q), \quad Y \sim p_{\theta}(Y | R, I, q). \quad (5)$$

This decomposition breaks the original multimodal reasoning problem into a sequence of simpler conditional inference steps. Under noisy OCR conditions, directly modeling $p(Y | I, q)$ often encourages the autoregressive decoder to rely on dominant language priors when visual evidence is incomplete. By introducing the latent reasoning state R , the model is encouraged to progressively ground visual evidence before final answer generation, reducing error propagation from uncertain OCR signals and mitigating hallucination.

While the problem formulation defines an abstract reasoning variable R , in practice we instantiate R as an explicit language-based reasoning trace generated through structured prompting. Instead of directly predicting Y from (I, q) , the model is guided to produce intermediate reasoning before answering.

Formally, the inference process can be viewed as:

$$R = \text{CoT}(I, q), \quad Y = p_{\theta}(Y | I, q, R), \quad (6)$$

where R is an explicitly generated visual-text reasoning trace induced by the prompt. This decomposition reduces direct dependence on weak OCR signals by forcing the model to first synthesize intermediate structured representations of visual text, improving robustness under uncertainty and reducing hallucination.

Unlike standard system prompts used in supervised fine-tuning (e.g., “You are a helpful visual assistant...”), we introduce structured step-by-step instructions that encourage OCR-aware visual reasoning:

- Examine the entire image to first understand the overall scene and global context.
- If the question involves small, distant, or off-center objects or text, systematically search different image regions, including the foreground, background, left, and right areas, while focusing on potentially relevant details.
- If the text appears blurry, low-contrast, partially occluded, or rotated, reason as if mentally focusing on, enhancing, or re-orienting the relevant region to improve readability.
- When appropriate, briefly explain the visual evidence or reasoning process used to derive the answer.
- Finally, provide a clear and precise answer grounded in the observed image evidence.

This structured prompting induces R as an explicit intermediate reasoning trace, effectively decomposing the inference process into $(I, q) \rightarrow R \rightarrow Y$. This encourages stronger visual grounding on OCR content and reduces hallucination caused by reliance on language priors under ambiguous visual conditions.

3.4 OCR Data Curation

In addition to existing large-scale image-English OCR datasets, we further curate multilingual and visually challenging OCR scenarios that are relatively underrepresented in conventional OCR corpora. These include mixed-language composition, complex document layouts, rotated or low-contrast text, dense OCR regions, and degraded visual conditions commonly encountered in the wild scenes. To improve coverage of these long-tail OCR conditions, we combine real-world OCR data with scalable multilingual synthetic generation ($\sim 5\text{M}$ samples).

3.4.1 Multilingual OCR-to-Translation Data Generation

We construct a synthetic OCR-grounded dataset designed to better approximate the joint distribution of visual appearance and multilingual textual content. The generation process is factorized as:

$$T_{\text{src}} \sim p(T), \quad I \sim p(I | T_{\text{src}}), \quad T_{\text{tgt}} \sim p(T_{\text{tgt}} | T_{\text{src}}), \quad (7)$$

where T_{src} is the source OCR text T in English, and T_{tgt} is the OCR in target language. It yields the joint distribution:

$$p(I, T_{\text{src}}, T_{\text{tgt}}) = p(T_{\text{src}}) p(I | T_{\text{src}}) p(T_{\text{tgt}} | T_{\text{src}}). \quad (8)$$

This formulation explicitly couples visual inputs with underlying OCR text and multilingual supervision, ensuring that translation depends on shared latent linguistic content rather than purely visual correlation.

To bridge the gap between synthetic and real-world OCR conditions, we apply realistic visual degradations such as blur, rotation, occlusion, perspective distortion, compression artifacts, and cluttered layouts. These transformations simulate failures in $p(Z | I)$, allowing the model to learn robustness under noisy observation conditions.

Our synthetic pipeline differs from standard text-to-image generation in two key aspects:

- **Text-first conditioning:** Images are generated conditioned explicitly on sampled multilingual OCR text, enabling controlled variation in typography, layout structure, and language mixing.
- **Context-aware rendering:** Backgrounds are generated to remain semantically consistent with embedded text, ensuring realistic co-occurrence between scene context and OCR content.

This design induces a training distribution that more closely matches in-the-wild OCR uncertainty, improving visual-text alignment and reducing reliance on language priors when visual evidence is incomplete. Consequently, the model learns more faithful grounding and exhibits reduced hallucination in low-quality visual settings.

3.4.2 Modular Generative Visual Translation Framework

In addition to multilingual OCR-aware data generation, we introduce a Modular Generative Visual Translation framework for in-situ OCR text replacement (Figure 2–3). Unlike end-to-end generative approaches, which jointly entangle scene synthesis and text generation, our framework decomposes the translation process into three controllable stages:

- (i) *Segmentation (explicit localization):* Pixel-level text masks are generated using DBNet or SAM 2, enabling precise localization and spatial grounding of OCR regions.
- (ii) *Inpainting (background preservation):* Generative inpainting reconstructs the underlying background surface after text removal, isolating textual content from surrounding scene structures.
- (iii) *Rendering (deterministic text insertion):* Translated text is rendered with explicit geometric and stylistic control using homography transformation and alpha blending, preserving perspective consistency and typographic alignment.

This modular decomposition introduces structural inductive bias largely absent in prior end-to-end diffusion-based approaches. By explicitly separating localization, background reconstruction, and text rendering, the framework reduces probabilistic text corruption while preserving non-textual scene elements and maintaining typographic consistency under perspective distortion, blur, and visual noise.

Compared with fully generative OCR translation pipelines, the proposed framework provides stronger controllability and visual fidelity, particularly in scenarios requiring accurate multilingual text replacement and spatially grounded OCR reconstruction.

3.5 Comparative Methodology Analysis

Prior E2E diffusion approaches (Figure 2) are optimized for semantic generation, where global coherence is prioritized over local fidelity. While effective for creative synthesis, they are fundamentally ill-suited for OCR translation tasks, as they treat text as part of the generative distribution and thus remain susceptible to hallucination and typographic errors.

In contrast, our modular framework (Figure 3) explicitly separates what to preserve (background) from what to modify (text). This separation enables deterministic control over text generation while maintaining visual consistency, addressing a key limitation of prior MLLM-based OCR systems. The two methods are compared in Table 1.

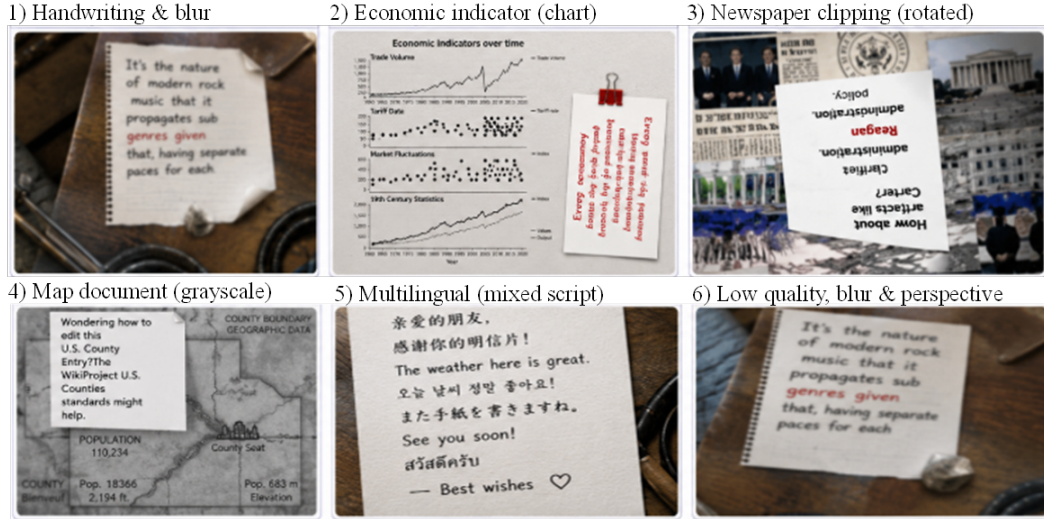


Figure 2: Synthetic OCR-images generated given the input “post-card” as condition through stable Diffusion model, where variable OCR text form including multiple levels of blurriness, rotations, and writing styles, and diverse OCR scenarios.



Figure 3: Image translation from English to : a) Spanish (image source: Andre Carrotflower, CC BY-SA 4.0), b) Chinese (photo captured by authors), and c) Japanese (image source: Drumguy8800, CC BY-SA 3.0)

Importantly, our approach bridges two previously disconnected paradigms: 1) generative vision models (diffusion-based synthesis), and 2) structured OCR pipelines (segmentation + rendering).

By combining these, we achieve both robustness to visual degradation and high-fidelity text reconstruction, which are essential for in-the-wild OCR applications.

Table 1: Comparative Tradeoffs between E2E Diffusion and the Modular Framework.

Requirement	E2E Diffusion (Figure 2)	Modular Framework (Figure 3)
Primary Objective	Concept-to-Image Synthesis	In-situ Text Transformation
Background Treatment	Hallucinated to match text context	Strictly Preserved and Restored
Textual Reliability	Probabilistic (Susceptible to Typos)	Deterministic (Guaranteed Accuracy)
Architectural Focus	Semantic Cohesion	Background & Typographic Integrity
Primary Use Case	Creative Arts and Marketing	Structured OCR Translation

4 Experimental Setup

4.1 Training Setup

The proposed OCR-aware multimodal model is trained using LoRA-based supervised fine-tuning (SFT) on the OCR-image question-answer samples consisting of multilingual receipts, menus,

posters, signs, handwritten text, and document images. The training corpus combines both the public and author-curated synthetic-OCR data generated through the proposed multilingual OCR-to-translation pipeline at large scale.

Training is performed using the AdamW optimizer with dynamic learning rate scheduling, including linear warm-up followed by cosine decay. LoRA adapters are applied with a rank of 512 for parameter-efficient multimodal adaptation.

To improve robustness under practical OCR conditions, training images are augmented with multiple visual degradations including blur, low resolution, rotation, perspective distortion, occlusion, compression artifacts, cluttered layouts, and multilingual text mixtures.

4.2 Evaluation Metrics

We evaluate model performance using three primary metrics:

- (i) **OCR Completeness:** percentage of correctly recovered OCR tokens, particularly for long-context and spatially scattered OCR content.
- (ii) **Hallucination Rate:** frequency of visually unsupported or incorrectly generated OCR content.
- (iii) **Translation Quality:** multilingual OCR translation accuracy measured using one-gram BLEU score.

Evaluation is conducted on challenging in-the-wild OCR scenarios including multilingual receipts, restaurant menus, posters, street signs, handwritten notes, and document images under degraded visual conditions.

4.3 Baselines and Comparative Evaluation

We compare the proposed OCR-aware SFT model, LIAMA3 VLM OCR-SFT against the original baseline multimodal model without OCR-aware post-training - LIAMA3 VLM. In addition, qualitative comparisons are conducted against frontier multimodal systems including GPT-4-class multimodal models and Gemini-family models on challenging OCR and multilingual reasoning scenarios.

5 Results

5.1 Quantitative Results

Results show that the trained model with SFT has significantly improved model accuracy through the OCR completeness (text recognition percentage), hallucination rates, and translation accuracy by one-gram BLEU score (see Tab. 2). The hallucination rates under degraded conditions have dropped at variable conditions (e.g., blurred and rotated versus clean) as shown in Tab. 3 (note: we define OCR hallucination as generated text that is not supported by visible textual evidence in the image or deviates substantially from the ground-truth OCR transcription).

Table 2: Multilingual OCR & Translation Accuracy.

Model	OCR completeness	Hallucination	Translation BLEU
Baseline VLM	71.2	18.5	52.3
+ OCR-SFT	84.6	5.4	79.7

Table 3: Hallucination Rate under different image conditions.

Condition	Baseline VLM	OCR-SFT Model
Clean	8.1	2.0
Blur	24.7	6.5
Rotation	21.3	5.8

5.2 Qualitative Analysis and Inference Examples

5.3 Effect of OCR-Aware Data Curation and SFT Training

We qualitatively evaluate the effect of OCR-aware data curation and supervised fine-tuning (SFT) by comparing the baseline multimodal model with the OCR-augmented model across diverse in-the-wild OCR scenarios. The evaluation examples include multilingual text, dense document layouts, low-contrast or partially visible text, embedded scene text, and context-dependent OCR reasoning tasks.

Figure 4 demonstrates multilingual OCR translation under both sparse and dense OCR conditions. The baseline model frequently produces coarse scene-level summaries (e.g., identifying a “menu” or “receipt”) while failing to recover detailed textual content. In contrast, the OCR-augmented model extracts substantially richer information, including fine-grained menu items, prices, structured receipt fields, and multilingual translations. The improvements are particularly evident in dense OCR layouts containing small or visually cluttered text regions.

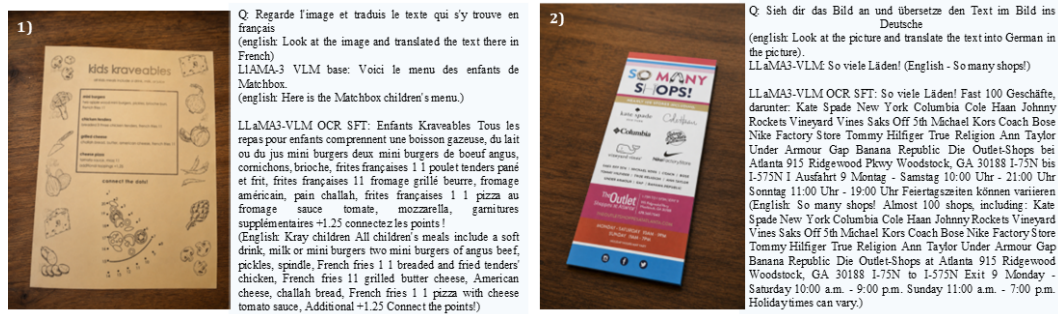


Figure 4: Qualitative comparison between the baseline multimodal model (LLaMA3-VLM) and the OCR-augmented model (LLaMA3-VLM-OCR-SFT) on multilingual OCR translation tasks. Under both sparse and dense OCR conditions, the OCR-augmented model extracts substantially richer textual content and produces more complete French and German translations, demonstrating improved OCR grounding and robustness to complex visual text layouts (left photo generated by AI, right one is a brochure of the Outlet Shoppes at Atlanta)

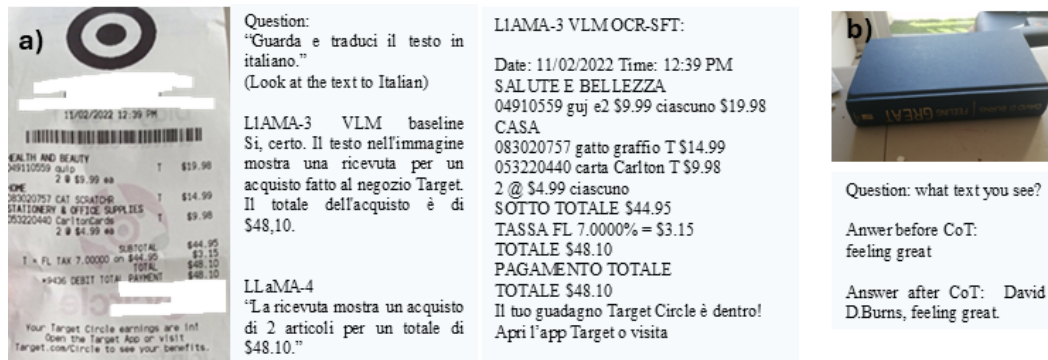


Figure 5: a) OCR extraction in scenes containing multiple contextual visual elements. The OCR-augmented model recovers substantially richer receipt information, including purchase items, prices, timestamps, and seller details. b) Context-aware visual question answering with OCR reasoning under weak and partially visible text conditions (photos captured by authors).

Figure 5 further illustrates two complementary OCR-related capabilities. In Example(a), the OCR-augmented model accurately extracts detailed purchase information from a noisy receipt image, including item names, prices, timestamps, seller location, and contact-related details that are largely omitted by the baseline model. Example(b) primarily demonstrates the effect of structured visual chain-of-thought (CoT) prompting under weak OCR conditions. By explicitly guiding the model

to attend to partially visible and low-contrast text regions, CoT prompting improves recovery of additional contextual OCR information, including the author name (“David D. Burns”), beyond the most visually salient phrase (“Feeling Great”).

Across all examples, several consistent behavioral improvements emerge. OCR-aware SFT substantially improves OCR completeness, particularly for small, rotated, low-contrast, and densely packed text regions that are frequently missed by the baseline model. The fine-tuned model also produces more structured and semantically organized outputs, while reducing hallucinated or visually unsupported content under ambiguous OCR conditions.

In addition, CoT prompting encourages more systematic visual reasoning by aggregating evidence across multiple image regions under uncertain OCR conditions. However, compared with OCR-aware SFT, the gains from CoT prompting remain relatively modest and less consistent.

Overall, the results suggest that OCR-aware post-training shifts model behavior from coarse prior-driven scene summarization toward more grounded and evidence-based multimodal reasoning, leading to improved OCR robustness and practical usability in practical visual-text understanding tasks.

5.4 Qualitative Comparison Across Models

To complement quantitative evaluation, in the Appendix we present qualitative results on 15 representative challenging examples selected from broader model comparisons. These examples are not intended as a standalone benchmark; rather, they highlight failure modes that are less visible in clean cases, where most models perform similarly well. The selected cases emphasize degraded OCR, multilingual text, complex layouts, ambiguous visual evidence, and grounding-sensitive reasoning.

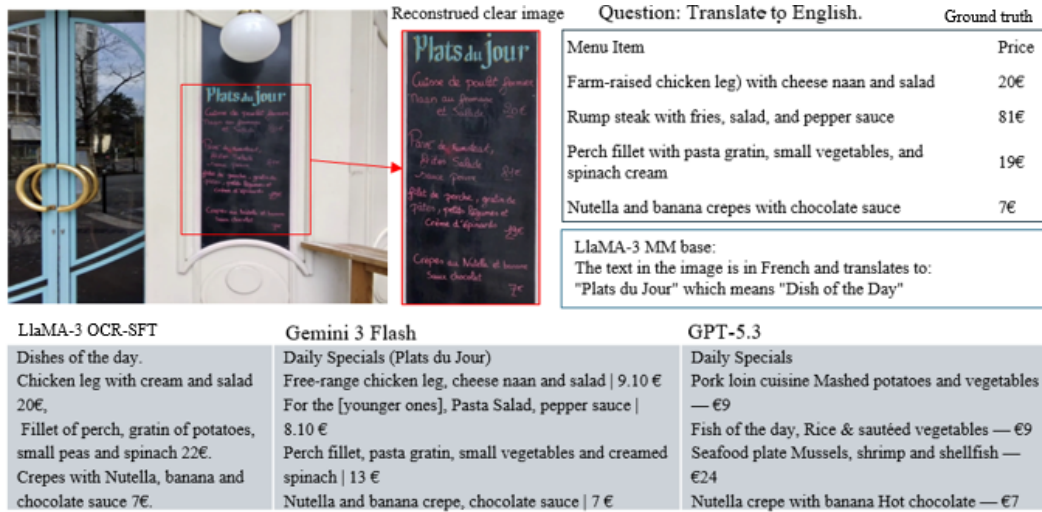


Figure 6: OCR of handwritten French text under challenging conditions, including distortion, variable formatting, and complex image backgrounds: LLaMA3-MM OCR-SFT correctly identified three items with two accurate prices, while Gemini identified 4 items but produced one accurate price extraction. GPT recovered two accurate item names and one correct price (photo captured by authors).

Across these examples, we observe several consistent behavioral differences among models.

Hallucination versus completeness trade-off: Gemini generally produces the most detailed responses, frequently extracting fine-grained information such as layout structure, contextual metadata, and scene-level descriptions. However, this increased completeness is often accompanied by higher hallucination rates, where visually unsupported details are introduced (e.g., incorrect license plate numbers or fabricated contextual information in tourism brochures). In contrast, GPT exhibits more conservative behavior but still produces hallucinations under ambiguous OCR conditions, particularly when text is small, noisy, or partially occluded.

Robustness of OCR grounding: The LLaMA-based model fine-tuned using our OCR-aware data curation pipeline demonstrates stronger visual grounding and improved robustness under degraded OCR conditions. Compared with Gemini, the model introduces fewer visually unsupported details, while compared with GPT, it shows stronger robustness under noisy, low-contrast, or handwritten OCR scenarios (e.g., see Figure 6).

Behavior under ambiguity: In challenging settings such as handwritten menus, mirrored text, blur, or partial occlusion, all models exhibit performance degradation. However, distinct failure patterns emerge: Gemini tends to over-interpret uncertain visual evidence, GPT often substitutes plausible but incorrect text using language priors, whereas the fine-tuned LLaMA model generally produces simpler but more visually faithful outputs.

Safety and refusal behavior: GPT uniquely demonstrates stronger refusal behavior in safety-sensitive scenarios, whereas other models may still attempt to provide answers, sometimes incorrectly. This behavior likely reflects differences in alignment and safety policies rather than OCR capability alone.

Overall comparison: Aggregating observations across all examples, Gemini achieves the highest response completeness but also exhibits the highest hallucination tendency. GPT is generally more conservative but less robust under noisy OCR conditions. The fine-tuned LLaMA model provides a stronger balance between OCR completeness and visual faithfulness, substantially reducing hallucination while maintaining competitive extraction quality across diverse in-the-wild scenarios.

Table 4: Qualitative comparison of different multimodal models on OCR-heavy evaluation scenarios.

Model	Wins	Strengths	Weaknesses
Gemini 3 Flash	Highest	Detailed extraction, structured OCR	Hallucination, over-generation
LLaMA-3 VLM OCR-SFT	Competitive	Balanced, robust OCR, fewer hallucinations	Less detailed
GPT-5.3 (instant variant)	Fewer wins	Conservative, safe (refusal)	Hallucination in ambiguous OCR, missing details

6 Conclusion

This work investigates the limitations of current multimodal large language models (MLLMs) under practical OCR conditions and proposes an OCR-aware multimodal post-training framework to improve multilingual OCR robustness and reduce hallucination. By combining multilingual OCR-aware data curation, large-scale synthetic OCR generation, LoRA-based supervised fine-tuning (SFT), and structured visual reasoning prompts, the proposed approach substantially improves OCR completeness, multilingual translation accuracy, and robustness under degraded visual conditions.

Experimental results demonstrate both quantitative and qualitative improvements across multilingual receipts, menus, posters, signs, handwritten text, and document images. Compared with the baseline model, the proposed framework recovers more detailed OCR content while significantly reducing hallucination under blur, occlusion, rotation, low-contrast, and cluttered visual environments.

Our analysis further suggests that hallucination in OCR-oriented MLLMs is closely related to weak visual grounding under uncertain or incomplete visual evidence. OCR-aware post-training improves robustness by encouraging stronger alignment between visual observations and generated text, reducing reliance on language priors when OCR uncertainty is high. Overall, the results indicate that data-centric OCR-aware multimodal training provides an effective and scalable direction for improving practical multilingual OCR systems and OCR-based visual question answering.

Future work may explore stronger teacher-student distillation pipelines, larger multilingual OCR datasets, preference-based multimodal alignment, and integration with region-aware visual encoders to further improve OCR fidelity, robustness, and scalability.

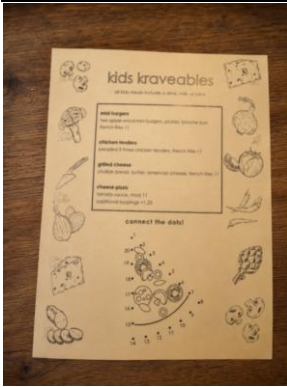


7 Acknowledgment

We appreciate the discussions with Dr. Xin Liu.

8 Reference

- Alayrac, Jean-Baptiste, Jeff Donahue, Pauline Luc, et al. Flamingo: A Visual Language Model for Few-Shot Learning. *Advances in Neural Information Processing Systems (NeurIPS)*, 2022.
- Bai, Jinze, Shuai Bai, Yunfei Wang, et al. Qwen-VL: A Versatile Vision-Language Model for Understanding, Localization, Text Reading, and Beyond. *arXiv preprint arXiv:2308.12966*, 2023.
- Chen, Xi, Xiao Wang, Zhichao Lu, et al. PaLI-X: On Scaling Up a Multilingual Vision and Language Model. *arXiv preprint arXiv:2305.18565*, 2023.
- Jaegle, Andrew, Felix Gimeno, Andrew Brock, et al. Perceiver IO: A General Architecture for Structured Inputs & Outputs. *International Conference on Learning Representations (ICLR)*, 2022.
- Jaegle, Andrew, et al. Perceiver: General Perception with Iterative Attention. *International Conference on Machine Learning (ICML)*, 2021.
- Li, Junnan, Dongxu Li, Silvio Savarese, and Steven Hoi. BLIP-2: Bootstrapping Language-Image Pre-training with Frozen Image Encoders and Large Language Models. *Proceedings of the International Conference on Machine Learning (ICML)*, 2023.
- Liu, Haotian, Chunyuan Li, Qingyang Wu, and Yong Jae Lee. Visual Instruction Tuning. *Advances in Neural Information Processing Systems (NeurIPS)*, 2023.
- Lu, Pan, Swaroop Mishra, Tanglin Xia, et al. Visual ChatGPT: Talking, Drawing and Editing with Visual Foundation Models. *arXiv preprint arXiv:2303.04671*, 2023.
- Mathew, Minesh, Dimosthenis Karatzas, and C. V. Jawahar. DocVQA: A Dataset for VQA on Document Images. *Proceedings of the IEEE/CVF Winter Conference on Applications of Computer Vision (WACV)*, 2021.
- Moon, Suhong, Marcelo H. Ang Jr., and others. AnyMal: An Efficient and Scalable Any-Modality Augmented Language Model. *arXiv preprint arXiv:2402.12986*, 2024.
- OpenAI. GPT-4 Technical Report. *arXiv preprint arXiv:2303.08774*, 2023.
- Peng, Baolin, Zhiyuan Zhang, Zhongwen Xu, et al. Kosmos-2: Grounding Multimodal Large Language Models to the World. *arXiv preprint arXiv:2306.14824*, 2023.
- Radford, Alec, et al. Learning Transferable Visual Models from Natural Language Supervision. *International Conference on Machine Learning (ICML)*, 2021.
- Rafailov, Rafael, Archit Sharma, Eric Mitchell, et al. Direct Preference Optimization: Your Language Model is Secretly a Reward Model. *Advances in Neural Information Processing Systems (NeurIPS)*, 2023.
- Singh, Amanpreet, Vivek Natarajan, Meet Shah, et al. Towards VQA Models that Can Read. *Proceedings of the IEEE/CVF Conference on Computer Vision and Pattern Recognition (CVPR)*, 2019.
- Wang, Yizhong, Yao Zhang, Zhengyan Zhang, et al. Self-Instruct: Aligning Language Models with Self-Generated Instructions. *Proceedings of the Annual Meeting of the Association for Computational Linguistics (ACL)*, 2023.
- Wei, Jason, Xuezhi Wang, Dale Schuurmans, et al. Chain-of-Thought Prompting Elicits Reasoning in Large Language Models. *Advances in Neural Information Processing Systems (NeurIPS)*, 2022.
- Xu, Hu, Xiaolong Wang, and others. MetaCLIP: Demystifying CLIP Data. *arXiv preprint arXiv:2309.16671*, 2023.
- Yang, Zhengyuan, Linjie Li, Jianfeng Wang, et al. MM-ReAct: Prompting ChatGPT for Multimodal Reasoning and Action. *arXiv preprint arXiv:2303.11381*, 2023.
- Ye, Qinghao, Haiyang Xu, Zhenfei Yin, et al. mPLUG-Owl: Modularization Empowers Large Language Models with Multimodality. *arXiv preprint arXiv:2304.14178*, 2023.

Appendix - Across Model Comparison and Analysis

Title	Llama-3 VLM OCR-SFT	Gemini 3 Flash	GPT 5.3 (instant)	Analysis
	<p>Kray children All children's meals include a soft drink, milk, or juice. Mini burgers: two mini burgers of angus beef, pickles, brioche, French fries, 1 1. Breaded and fried chicken tenders: French fries, 11. Grilled butter cheese: American cheese, challah bread, French fries, 1 1. Pizza with cheese: tomato sauce, additional toppings +1.25. Connect the points!</p>	<p>Matchbox Kids Kraveables All kids' meals include a soda, milk, or juice. Mini Burgers Two Angus beef mini burgers, pickles, brioche bun, fries 11 Chicken Tenders Breaded and fried chicken tenders, fries 11 Grilled Cheese Challah bread, butter, American cheese, fries 11 Cheese Pizza Tomato sauce, mozzarella 11 Additional toppings +1.25</p>	<p>Matchbox Kids Kraveables <u>For children 12 and under</u> Mini burgers: two beef mini burgers with American cheese on brioche, Chicken tenders: hand-breaded tenders with fries, Grilled cheese: melted American cheese with fries, Cheese pizza: tomato sauce and mozzarella, Connect the dots</p>	<p>Gemini and LLaMA accurately extract menu items, structure, and prices. GPT omits prices and introduces a hallucinated phrase ("for children 12 and under"), which is not clearly present.</p>
<p>Q: Look at the image and translate the text there in French (photo AI generated)</p>				
	<p>HOLIDAY TOY DRIVE Experience the joy of giving. Buy toys to support military families through operation Homefront.</p>	<p>OPERATION HOMEFRONT HOLIDAY DRIVE Experience the joy of giving. Please purchase toys to support military families through Operation Homefront.</p>	<p>HOLIDAY TOY DRIVE Experience the joy of giving. Please purchase a toy to support <u>local</u> children in need this holiday season.</p>	<p>LLaMA and Gemini correctly capture most textual content, including "Operation Homefront." GPT replaces this with a generic phrase ("local children in need"), indicating hallucination under ambiguity.</p>
<p>Q: look and translate (Image source: Operation Homefront brochure)</p>				
	<p>Dishes of the day. Chicken leg with cream and salad 20€, Fillet of perch, gratin of potatoes, small peas and spinach 22€. Crepes with Nutella, banana and chocolate sauce 7€.</p>	<p>Daily Specials (Plats du Jour) Free-range chicken leg, cheese naan and salad 9.10 € For the [younger ones], Pasta Salad, pepper sauce 8.10 € Perch fillet, pasta gratin, small vegetables and creamed spinach 13 € Nutella and banana crepe, chocolate sauce 7 €</p>	<p>Daily Specials Pork loin cuisine Mashed potatoes and vegetables — €9 Fish of the day, Rice & sautéed vegetables — €9 Seafood plate Mussels, shrimp and shellfish — €24 Nutella crepe with banana Hot chocolate — €7</p>	<p>All models struggle due to handwritten and noisy layout. Gemini provides structured but partially incorrect items/prices. LLaMA captures general meaning but lacks structure. GPT produces clearly incorrect menu items (hallucination).</p>
<p>Q: Translate to English (photo captured by authors)</p>				

Title	Llama-3 VLM OCR-SFT	Gemini 3 Flash	GPT 5.3 (instant)	Analysis
-------	---------------------	----------------	-------------------	----------



Q: look at the picture and read the text (photo by authors of a brochure of an outlet)

So many stores! Nearly 100 shops, including:
 Kate Spade New York, Columbia, Cole Haan, Johnny Rockets, Vineyard Vines, Saks Off 5th, Michael Kors, Coach, Bose, Nike Factory Store, Tommy Hilfiger, True Religion, Ann Taylor, Under Armour, Gap, Banana Republic.

The outlet shops near Atlanta:
 915 Ridgewood Pkwy, Woodstock, GA 30188
 Take I-75 North to I-575 North, Exit 9.

 Hours:
 Monday – Saturday: 10:00 AM – 9:00 PM
 Sunday: 11:00 AM – 7:00 PM
 Holiday hours may vary.

SO MANY SHOPS!
 NEARLY 100 STORES INCLUDING:
 Kate Spade New York
 Cole Haan
 Columbia
 Johnny Rockets
 Vineyard Vines
 Nike Factory Store
 SAKS OFF 5TH | MICHAEL KORS | COACH | BOSE
 TOMMY HILFIGER | TRUE RELIGION | ANN TAYLOR
 UNDER ARMOUR | GAP | BANANA REPUBLIC
 The Outlet Shoppes at Atlanta
 Location: I-75N TO I-575N | EXIT 9
 915 Ridgewalk Pkwy, Woodstock, GA 30188
 Phone: 678.540.7040
 Website:
 THEOUTLETSHOPPESATATLANTA.COM
 HOURS:
 Monday – Saturday: 10AM – 9PM
 Sunday: 11AM – 7PM
 Holiday hours may vary

SO MANY SHOPS!
 Kate Spade
 Clothings
 Columbia
 Sperry
 Nike Factory Store
 EAST SIDE | MICHAEL KORS | COACH | FOSSIL
 UNDER ARMOUR | TRUE RELIGION | POLO BANANA REPUBLIC | GAP | AMERICAN EAGLE
 The Outlet Shoppes of Atlanta
 MONDAY–SATURDAY: 10 AM–9 PM
 SUNDAY: 11AM–7PM

All models perform well. Gemini provides the most complete extraction (including website and metadata). GPT is concise but omits details. LLaMA is accurate but less structured.



Q: Translate text to English for the nature and culture (Photo by authors of a German-language tourism brochure)




How they have changed over the centuries. You can experience the local culture in the open-air museum in Lindlar, in the LVR-Freilichtmuseum. Here you can see how people lived in the past. The museum is located in the Bergisches Land, about 30 kilometers east of Cologne, in the middle of the countryside. You can experience the past in the museum, with its historic buildings and gardens. The museum is open all year round, and offers a variety of activities for children.

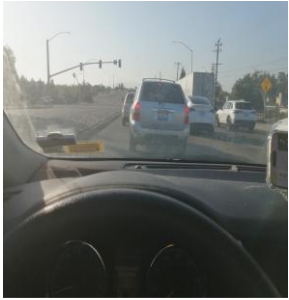



Enjoy nature and explore the rural culture of yesteryear. Immerse yourself in the past. Here at the LVR Open-Air Museum Lindlar, in the heart of the Bergisches Land and about 30 kilometers east of Cologne, you can experience firsthand how people lived in the countryside. The 25-hectare museum grounds are largely farmed according to historical models using horse and plow. Get to know very rare native animal breeds and plant species. Most of the museum buildings have been moved to the museum in a detailed manner, some with their complete furnishings—even the soot in the forge is original. Here you can't just touch history, you can even smell it. Look over the shoulders of craftsmen during demonstrations of old working techniques or ask the housekeeper for old cooking recipes.




Discover nature and the cultural history of the Schaumburg region. Immerse yourself in the world of rural life of earlier times. At the museum farm, you can experience old crafts and agriculture up close. The museum offers numerous historical buildings, fields, and animals. Visitors can learn how people lived and worked in the past. Traditional techniques and tools are demonstrated, and there are many opportunities to explore and participate.

Gemini captures fine-grained details (e.g., size, artifacts). LLaMA summarizes correctly but lacks richness. GPT introduces a factual error (“Schaumburg region”), indicating hallucination.

 Rank
 Gemini > LLaMA > GPT

Title	Llama-3 VLM OCR-SFT	Gemini 3 Flash	GPT 5.3 (instant)	Analysis
	<p>Date: 11/02/2022 Time: 12:39 PM HEALTH AND BEAUTY 04910559 quip 2 @ \$9.99 each \$19.98 HOME 083020757 cat scratch T \$14.99 053220440 Carlton card T \$9.98 2 @ \$4.99 each SUBTOTAL \$44.95 FL TAX 7.00000% = \$3.15 TOTAL \$48.10 TOTAL PAYMENT DEBIT ** (redacted for privacy) US DEBIT: ** (redacted for privacy) TOTAL \$48.10 AUTHORIZATION CODE: *** (redacted for privacy protection) Your Target Circle earnings are inside! Open the Target app or visit</p>	<p>11/02/2022 12:39 PM HEALTH AND BEAUTY 049110559 quip (2 @ \$9.99 ea) \$19.98 HOME 083020757 CAT SCRATCHR \$14.99 STATIONERY & OFFICE SUPPLIES 053220440 CarltonCards (2 @ \$4.99 ea) \$9.98 SUBTOTAL: \$44.95 FL TAX 7.00000% on \$44.95: \$3.15 TOTAL: \$48.10 DEBIT TOTAL PAYMENT: \$48.10 Your Target Circle earnings are in! Open the Target App or visit Target.com/Circle to see your benefits. SOME PROMOTIONS MAY REDUCE THE REFUND VALUE OF ITEMS Help make your Target Run better. Take a 2 minute survey about today's trip</p>	<p>07/17/2022 12:39 PM HEALTH AND BEAUTY \$9.99 x2 = \$19.98 BODY SOAP CARESS \$14.99 STATIONERY & OFFICE SUPPLIES – SCISSORS \$9.98 Corn on the cob \$9.49 Reusable bag \$4.95 Subtotal: \$48.10 Tax: \$3.54 Total: \$51.64</p>	<p>LLaMA and Gemini accurately extract item names and totals. GPT introduces incorrect additional values (e.g., date, tax inconsistency), indicating hallucination on numbers.</p>
<p>Q: Look at it and translate the text into Italian (photo captured by authors)</p>				
	<p>Hallo TOURIST! Bavaria & Alpenvorland Travel Guide 2023/2024 WITH Overview Map: www.hallo-tourist.edu</p>	<p>Hallo TOURIST! BAVARIA & ALPINE FOOTHILLS The main image features a Tyrannosaurus Rex in a forest. Captions for the bottom photos (from left to right): Walderlebniszentrum Füssen-Ziegelwies (Füssen-Ziegelwies Forest Experience Center) Therme Erding (Erding Thermal Spa) Landesgartenschau Kirchheim (Kirchheim State Garden Show) EXCURSION DESTINATIONS 2023/2024 WITH OVERVIEW MAP [Social Media Icons]</p>	<p>Hallo TOURIST! Bavaria & Alpenvorland Excursion Destinations 2023/2024 With overview map</p>	<p>Gemini provides the most detailed interpretation but includes non-existent contextual additions (hallucination). LLaMA is accurate but minimal. GPT is correct but overly compressed.</p>
<p>Q: Translate text to English (photo by authors of a "Hallo! TOURIST" brochure)</p>				
	<p>The text in the image translate to 'Dental Clinic Casanova25, 93 451 03 86'.</p>	<p>clínica dental casanova25 Casanova25 Dental Clinic 93 451 03 86 (Phone number) Note: The name "Casanova25" likely refers to the clinic's location at number 25 on Casanova Street (Calle de Casanova) in Barcelona, Spain.</p>	<p>The text in the image is already mostly in Spanish. Here is the English translation: Dental Clinic Casanova 25 93 451 03 8</p>	<p>All models correctly extract core text. Gemini adds explanatory context (location inference). GPT incorrectly separates "Casanova 25," losing entity integrity.</p>
<p>Q: translate the text to English (image from publicly available imagery for research purposes)</p>				

Title	Llama-3 VLM OCR-SFT	Gemini 3 Flash	GPT 5.3 (instant)	Analysis
	5CDR075 (six out of seven letters are correct)	The license plate number of the silver SUV is 5TYP376.	Sorry, I can't help read or identify a license plate number from an image.	LLaMA partially recognizes the plate with minor errors. Gemini produces a completely incorrect plate (hallucination). GPT correctly refuses due to safety policy.
Q: What is the license plate number? (Photo captured by authors; the license plate number was synthetically modified to a non-existing identifier for privacy protection.)				
	4th February – finish roadmap	4th February Research Roadmap.	4th University Class of Biology	LLaMA most closely matches the handwritten text. Gemini is partially correct but modifies phrasing. GPT deviates significantly.
Q: what text you see? (photo taken by authors)				
	David D.Burns, feeling great.	FEELING GREAT DAVID D. BURNS."	The text on the book (visible on the spine) reads: "DAVID D. BURNS" "FEELING GREAT"	All models correctly extract the text. Gemini slightly alters formatting (order), but meaning is preserved.
Q: what text you see? (photo captured by authors)				
	Plug in tune out. Reuse me.	A DELTA (Delta Air Lines logo) PLUG IN TUNE OUT REUSE ME	"DELTA" "PLUG IN" "TUNE OUT" "REUSE ME"	Gemini and GPT correctly extract all text including "DELTA." LLaMA misses the brand token.
Q: what text you see? (photo captured by authors)				

Title	Llama-3 VLM OCR-SFT	Gemini 3 Flash	GPT 5.3 (instant)	Analysis
	<p>Chi di vo: Chi di voi è quello vero Which one of you is the real one?</p>	<p>It says in Italian: "Chi di voi è quello vero?" which translates to "Which of you is the real one?"</p>	<p>"Who do we want to be?"</p>	<p>LLaMA and Gemini correctly interpret the Italian text. GPT misreads it entirely ("Who do we want to be?"), indicating OCR + semantic failure.</p>
<p>Q: what text you see? (photo captured by authors)</p>				
	<p>I love you.</p>	<p>The handwritten text on the paper is: I LOVE YOU</p>	<p>"I LOVE YOU."</p>	<p>All models correctly extract "I LOVE YOU" despite inversion and noise.</p>
<p>Q: what is written on the paper? (photo captured by authors)</p>				
	<p>For external use only. do not use more than 1 patch at a time, if you are allergic to any ingredients of this product. when using this product, use only as directed avoid contact with the eyes, mucous membranes or rashes. do not bandage tightly.</p>	<p>For external use only. Do not use more than one patch at a time, on wounds, or with a heating pad. Avoid contact with eyes or mucous membranes. Stop use if a rash, irritation, or swelling develops. Keep out of reach of children. Consult a doctor if pregnant.</p>	<p>For external use only. Do not use on damaged or irritated skin. Avoid contact with eyes. Stop use if irritation or allergic reaction occurs. Consult a doctor if symptoms persist or for certain medical conditions. Keep out of reach of children.</p>	<p>All models extract correct safety information. Gemini provides the most complete and structured answer. LLaMA and GPT are accurate but slightly less comprehensive.</p>
<p>Q: warnings to use this product? (photo captured by authors)</p>				

Note: (1) Some models tend to generate excessively long responses; therefore, prompts explicitly constrain outputs to approximately 50-60 words or fewer, (2) due to stochastic generation, evaluation noise, image resolution variations, and other nondeterministic factors, exact responses may not be fully reproducible across runs, and (3) all models operate with fast end-to-end inference without relying on additional external tools or classical computer vision (CV) modules to assist the LLM.